Journal of Engineering Mathematics **31:** 131–142, 1997.

An efficient storage scheme for reduced chemical kinetics based on orthogonal polynomials

H. NIEMANN[1], D. SCHMIDT[1]* and U. MAAS[2]
[1]*Interdisziplinäres Zentrum für Wissenschaftliches Rechnen, Universität Heidelberg Im Neuenheimer Feld 368, 69120 Heidelberg, Germany; e-mail: schmidt@itv.uni-stuttgart.de*
[2]*Konrad-Zuse-Zentrum für Informationstechnik, Heilbronner Str. 10, 10711 Berlin, Germany*

Received 18 March 1996; accepted in revised form 13 November 1996

Abstract. Simplified chemical kinetic schemes are a crucial prerequisite for the simulation of complex three-dimensional turbulent flows, and various methods for the generation of reduced mechanisms have been developed in the past. The method of intrinsic low-dimensional manifolds (ILDM), *e.g.*, provides a mathematical tool for the automatic simplification of chemical kinetics, but one problem of this method is the fact that the information which comes out of the mechanism reduction procedure has to be stored for subsequent use in reacting-flow calculations. In most cases tabulation procedures are used which store the relevant data (such as reduced reaction rates) in terms of the reaction progress variables, followed by table look-up during the reacting-flow calculations. This can result in huge amounts of storage needed for the multi-dimensional tabulation. In order to overcome this problem a storage scheme is presented which is based on orthogonal polynomials. Instead of the use of small tabulation cells and local mesh refinement, the thermochemical state space is divided into a small number of coarse cells. Within these coarse cells polynomial approximations are used instead of frequently used multi-linear interpolation. This leads to a considerable decrease of needed storage. The hydrogen-oxygen system is considered as an example. Even for this small chemical system, a decrease of the needed storage requirement by a factor of 100 is obtained.

Key words: reduced chemical kinetics, tabulation of reduced kinetics, polynomials, laminar flames

1. Introduction

The interest in the numerical simulation of reacting flows has grown considerably during the last years. The underlying chemical kinetics of combustion processes is (at least for aliphatic hydrocarbons) adequately well understood [1], and numerical methods are available, which allow to couple chemical kinetics with flow and molecular transport. Numerical simulations of laminar flames in one- or two-dimensional configurations have become a standard tool in combustion research (see, *e.g.* [2, 3]). However, if one is interested in general, multi-dimensional, turbulent flames, a detailed treatment of the chemical and physical processes is, and will be in the near future, computationally prohibitive [4]. Thus, simplified models for the turbulence (see, *e.g.*, [4–6]), as well as for the chemical kinetics have to be devised.

The need of simplified models for the chemistry stems from the fact that for each chemical species (which can be more than 1000 in the low-temperature oxidation of higher hydrocarbons [7]) a species-conservation equation has to be solved. This is possible, if simple systems like spatially homogeneous ignition (*e.g.* in shock tubes) are simulated [1], but computationally prohibitive for other reacting flows.

Almost 100 years ago Bodenstein [8] observed that some chemical reactions are so fast that some chemical species in the reaction system are in a quasi-steady state. Based on the ideas of Bodenstein, many attempts have been made to develop simplified descriptions of chemical-

[*] Author for correspondence.

reaction systems, *e.g.*, for the simulation of complex combustion processes. A variety of different approaches can be found in the literature, such as systematically reduced mechanisms [9], the constrained equilibrium approach [10], computational singular perturbation [11, 12], repro-modelling [13], dynamic dimension reduction [14], or the method of intrinsic low-dimensional manifolds [15–17], to name only a few examples. Good surveys of current work can be found in [9, 18, 19]. In this work we shall present some new results of the implementation of reduced chemistry based on intrinsic low-dimensional manifolds (ILDM).

The scalar field of a reacting flow involving n_s species evolves in time according to an $(n_\psi = n_s + 2)$-dimensional system of partial differential equations

$$\frac{\partial \underline{\psi}}{\partial t} = \underline{F}(\psi) + \underline{\Xi}(\underline{\psi}, \nabla\underline{\psi}, \nabla^2\underline{\psi}). \tag{1}$$

In this equation $\underline{\psi} = (h, p, w_1/M_1, w_2/M_2, \ldots, w_{n_s}/M_{n_s})^{\mathrm{T}}$ denotes the vector of scalars with $h =$ specific enthalpy, $p =$ pressure, M_i the molar mass and w_i the mass fraction of the species i. $\underline{F}(\underline{\psi})$ denotes the vector of chemical reaction rates, and $\underline{\Xi}(\underline{\psi}, \nabla\underline{\psi}, \nabla^2\underline{\psi})$ the vector describing all the physical processes, such as convection, diffusion, heat conduction, etc.

The ILDM-approach [15, 16], as well as all the other approaches, uses the fact that in typical reaction systems a large number of chemical processes are so fast that they are not rate limiting and can be decoupled. All the method does is to identify intrinsic low-dimensional manifolds in the $(n_\psi = n_s + 2)$-dimensional state space with the property that after a short relaxation time the thermochemical state of the system has relaxed onto these attracting low-dimensional manifolds. Then the state of the chemical system is a known function of only a few N variables $\underline{\theta}$ which parameterize the manifold, *i.e.* $\underline{\psi} = \underline{\psi}(\underline{\theta})$, and the governing n_ψ-dimensional equation system (1) can be projected onto the N-dimensional subspace

$$\frac{\partial \underline{\theta}}{\partial t} = \underline{S}(\underline{\theta}) + \underline{\Gamma}(\underline{\theta}, \nabla\underline{\theta}, \nabla^2\underline{\theta}). \tag{2}$$

Thus, the ILDM-approach basically consists of three steps [15–17, 20]

- Identify the ILDM and obtain information about the coupling of the chemical kinetics with flow and molecular transport.
- Store the information, namely $\underline{\psi}(\underline{\theta})$ and the projection $\underline{\Xi} \rightarrow \underline{\Gamma}$ for subsequent use in the reacting-flow simulation.
- Solve the projected system of partial differential equation (2) for the scalar field.

Various examples have been treated and they have verified the approach [17, 20–24]. It turns out that the main remaining challenges in the implementation of the method are

- The efficient numerical calculation of the ILDM.
- A local adaption of the dimension of the manifolds based on the desired accuracy of the reduced scheme.
- The efficient storage of all the data needed for the subsequent use in the reacting flow calculation.

In this paper we address the third item, namely an efficient storage of the ILDM.

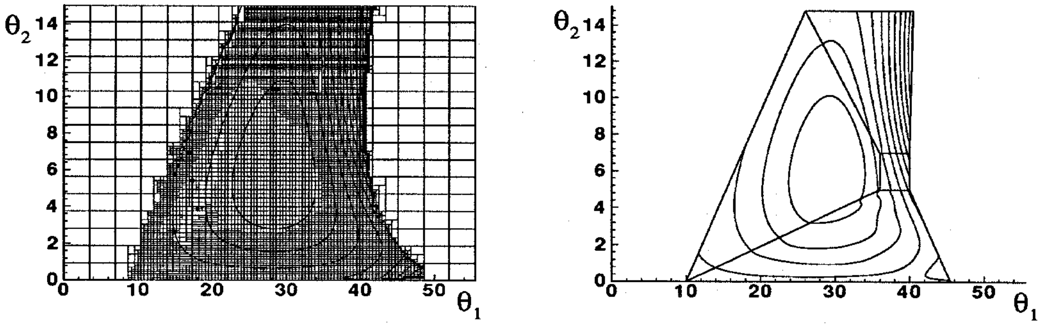

Figure 1. Different grid-types, isolines denote equal rates of formation of H_2O. (Left: Conventional storage scheme, Right: New storage scheme with coarse cells).

2. Polynomial storage scheme

2.1. Problem formulation

The implementation of ILDM-reduced chemistry in CFD-codes is based on the projection of the n_ψ-dimensional conservation equations for the scalar field onto the N-dimensional attracting ILDM. This procedure requires a knowledge of several properties of the reduced scheme, namely

- N rates $\underline{S}(\underline{\theta})$ for the reduced variables;
- the n_ψ state variables $\underline{\psi}(\underline{\theta})$ characterizing the manifold and
- and $N \times n_\psi$ entries of the projection operator $P(\underline{\theta})$ which describes the coupling of the chemistry with the physical processes.

Because the evaluation of the ILDM is quite time consuming, and the results are usually used in a large number of different CFD-calculations, the properties given above are usually calculated beforehand and stored in terms of the reduced state variables $\underline{\theta}$.

The storage scheme for the ILDM used up to now was based on a table-set-up procedure [16]. The tabulation region was predefined and an adaptive grid with local mesh refinement was used (see Figure 1). Within the grid cells multi-linear interpolation was used to calculate the properties from the values at the grid nodes. The disadvantage of this storage scheme is the huge size of these tables for future applications. If we are thinking of modelling real diesel-engine combustion, at least 3 reaction progress variables are needed. Additionally the parameters pressure, enthalpy and mixture fraction have to be varied as tabulation coordinates, leading to a table with tabulating dimension at least $N = 6$. Considering a case where about 1000 species are taking part in the reactions with at least 10 grid points being used in each tabulation direction, we end up with about 10^9 numbers to be stored. This table cannot be handled. The problem gets worse, if we account for differential diffusion, adding element composition variables to the set of reduced variables. From this it can be seen that an efficient storage of the reduced mechanism is crucial for its use in CFD-codes, and several approaches alternative to the tabulation have been pursued (see, *e.g.*, [13, 25, 26]).

We start the development of our storage procedure based on two observations

- It is evident that, if we replace the multi-linear interpolation in the grid cells by higher-order polynomial, the accuracy is improved considerably.

- If we use the tabulation procedure outlined above [16], it is inevitable that the refinement is based on all the different properties which have to be stored. Thus, the property with the worst local behavior defines the local grade of refinement, though all other properties might have a smooth behavior. A solution to overcome this is to use different interpolating functions for each property with adaptive complexity and order.

Multidimensional polynomials are the most simple functions to use. They can be evaluated efficiently with Horner schemes. The idea to use polynomials for approximation of chemical-reaction-rate data is shown in [25]. An overview of the literature can be found there, too. However, this approach has some disadvantages: The use of only one polynomial for the whole tabulation domain usually requires a very high order of the polynomial. This will lead to numerical problems in every fitting algorithm. If this problem is circumvented by dividing the tabulation domain into sub-domains and fitting the different sub-domains with their own low-grade polynomials, we observe that the properties are not continuous at the cell boundaries. This leads to problems in using the table in CFD-codes, especially when gradient based solvers are used.

In order to overcome these deficiencies, we develop a procedure, which divides the whole state space into sub-domains (represented by coarse cells, *cf.* Figure 1), uses medium-grade polynomials within these cells, and additionally ensures continuity at the boundaries of the cells. The approximating polynomials are computed independently for each cell. This enhances the flexibility of the table set-up and enables a parallelization of the tabulation code.

2.2. Coarse grid and local coordinates

Let us start the analysis with a brief survey of the nomenclature that we have adopted. The manifold is given as a subset $\mathcal{M}$ of the state space with

$$\mathcal{M} = \{\underline{\psi}(\underline{\theta}) \mid \underline{\theta} \in \mathcal{D}\}, \tag{3}$$

where $\underline{\theta} \to \underline{\psi}$ defines the mapping of the reduced variables onto the respective points of the manifolds, and $\mathcal{D}$ defines the domain of the reduced variables. The mappings $\underline{\theta} \to \underline{\psi}$ and $\underline{\psi} \to \underline{\theta}$, as well as the domain $\mathcal{D}$ are obtained during the generation of the ILDM. This will be the topic of another publication. In the following we assume explicitly that the mapping (the parameterization of the manifold) as well as $\mathcal{D}$ are known. Thus, in order to simplify the presentation, we start from a given manifold which has been obtained using a tabulation procedure [16]. As an example we use the ILDM of a hydrogen–oxygen system. The two-dimensional manifold is parameterized in terms of two reaction-progress variables $\theta_1 = w_{\mathrm{H_2O}}/M_{\mathrm{H_2O}}$ and $\theta_2 = w_{\mathrm{H}}/M_{\mathrm{H}}$, which are in the intervals $0 < \theta_1 < \theta_1^{\max}$ and $0 < \theta_2 < \theta_2^{\max}$. The conventional tabulation of the manifold is shown in the left part of Figure 1. The manifold is tabulated by a rectangular grid with local mesh refinement. Within the fine cells multilinear interpolation is used. The new storage scheme, allowing an efficient storage of the ILDM, is based on a division of the domain of the manifold into non-rectangular coarse cells, which can be seen in the right part of Figure 1. The accuracy requirement is then met by use of higher-order interpolation. Thus, fine grid cells with first-order interpolation in the old scheme are replaced by coarse grid cells with higher-order interpolation. For simplicity of the table lookup, it was decided to use coarse cells that can be mapped on rectangular cells. So the coarse cells have always 2^N corners (N is the tabulation dimension). The choice of the coarse cells can, of course, be guided by the information coming out of the mechanism-reduction

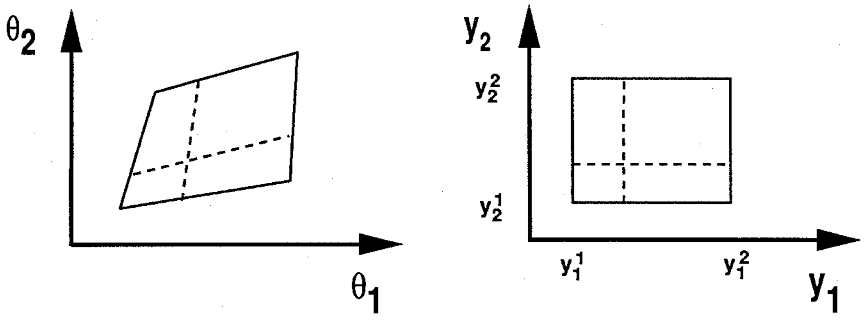

Figure 2. Transformation from global coordinates to local cell-coordinates.

procedure. For the example considered here we base the set-up of the coarse cells on the known behavior of the reaction rates (*cf.* Figure 1). Having specified the coarse cells, we establish the local coordinates in each cell by the mapping $\underline{\theta} \to \underline{y}$ of the cell on a rectangular cell with the coordinates $\underline{y}$, as shown in Figure 2. The cell is bounded by the cell coordinates y_i^1 and y_i^2, $i = 1, 2, \ldots, N$, and the cell is given by $\mathcal{S}^N = \{\underline{y} \,|\, y_i \in [y_i^1, y_i^2], i = 1, 2, \ldots, N\}$. The choice of the local corner coordinates y_i^1, y_i^2) is arbitrary in the mapping aspect.

The remaining task is now to find a polynomial representation of $\underline{S}(\underline{\theta}), \underline{\psi}(\underline{\theta})$ and $P(\underline{\theta})$ within the coarse cells with the additional constraint that the functions are continuous over the cell boundaries.

2.3. Polynomial interpolation within the coarse cells

2.3.1. *Ensuring continuous functions at the boundaries*

The idea behind making continuous functions between two neighbouring cells is to calculate a function on the shared boundary first, and then to use this boundary function for the calculation of the approximating function (cell function) within the cell. On the boundary the cell function is forced to degenerate to the boundary function. For the two-dimensional example shown in Figure 1 this means that we must calculate functions on the straight border lines first, and then fitting the area inside the cells.

Given an N-dimensional cell $\mathcal{S}^N$, we have $2N$ bounding hyperplanes $\mathcal{S}_i^{N-1}$, $i = 1, 2, \ldots,$ $2N$, which shall be denoted by $\mathcal{R}_i^j = \{\underline{y} \,|\, \underline{y} \in \mathcal{S}^N \wedge y_i = y_i^j\}, i = 1, 2, \ldots, N$, and $j = 1, 2$. On the bounding hyperplanes $(\underline{y} \in \mathcal{R}_i^j)$ the approximating functions shall be given by $b_i^j(\underline{y})$. In the cell the following *ansatz* is used for the approximating function $F(\underline{y})$

$$F(\underline{y}) = Z(\underline{y})L(\underline{y}) + B(\underline{y}). \tag{4}$$

On the boundaries $\mathcal{S}_i^{N-1}$ the function $Z(\underline{y})$ is forced to equal zero

$$Z(y) = \prod_{i=1}^{N} (y_i - y_i^1)(y_i - y_i^2). \tag{5}$$

There the *ansatz* (4) degenerates to $F(\underline{y}) = B(\underline{y})$. By defining the boundary function $B(\underline{y})$ such that $B(\underline{y}) = b_i^j(\underline{y})$ for all $\underline{y}$ in $\mathcal{R}_i^j$, we ensure continuity between cells. The calculation of $B(\underline{y})$ is somewhat tricky. It is based on the condition that the polynomials of $b_i^j(\underline{y})$ do not contain any powers of y_i, together with the condition that $B(\underline{y}) = b_i^j(\underline{y})$ for all $\underline{y}$ in $\mathcal{R}_i^j$. From this a recursion formula for the coefficients of the monomials can be obtained. The fitting in the interior cell is done by a serial expansion of $L(\underline{y})$ under the above constraints, so that the approximation error between $F(\underline{y})$ and some reference points from the ILDM is kept below a given limit.

2.3.2. *Calculation of the approximating polynomials*

The function $L(\underline{y})$ is calculated in a least-squares sense which minimizes the relative error between $F(\underline{y})$ and a set of reference points calculated inside the cell. Due to the previous calculation of $B(\underline{y})$ and its linear interpolation property less effort has to be taken in the least-squares step. This is especially helpful for the application on ILDM-tables, because the evaluation of points on the manifold is quite expensive, and the number of reference points needed to be calculated should be as small as possible.

The aim in calculating $L(\underline{y})$ is to reduce the average relative error between the function $F(\underline{y})$ and the values $p({}^i\underline{y})$ at the m reference points ${}^i\underline{y}$ below a given limit ε

$$\sum_{i=1}^{m} \left(\frac{F({}^i\underline{y}) - p({}^i\underline{y})}{p({}^i\underline{y})} \right)^2 < m\varepsilon^2. \tag{6}$$

This is achieved by a serial expansion of $L(y)$. For this, the following *ansatz* is used

$$L(y) = \sum_{j=1}^{k} a_j \phi_j(y). \tag{7}$$

Here $\phi_j(y)$ are the basis functions for the series. The a_j are coefficients that have to be adjusted in the least-squares step.

Introducing the serial expansion (7) into the *ansatz* (4) combined with the condition of minimizing the sum of the squared relative errors (6), we are led to the following linear system of equations from which to determine the k unknown coefficients a_l

$$\sum_{j=1}^{k} a_j \sum_{i=1}^{m} \left(\frac{B({}^i\underline{y})}{p({}^i\underline{y})} \right)^2 \phi_j({}^i\underline{y}) \phi_l({}^i\underline{y}) + \sum_{i=1}^{m} \left(\frac{B({}^i\underline{y})}{p({}^i\underline{y})} - 1 \right) \frac{Z({}^i\underline{y})}{p({}^i\underline{y})} \phi_l({}^i\underline{y}) = 0,$$
$$l = 1 \ldots k. \tag{8}$$

In the above form all k equations are coupled. A real expansion of the series in the sense of calculating all a_l independently one by one, until the required accuracy is achieved, seems to be computationally prohibitive. But defining a scalar product by

$$\langle \phi_j, \phi_l \rangle = \sum_{i=1}^{m} \left(\frac{B({}^i\underline{y})}{p({}^i\underline{y})} \right)^2 \phi_j({}^i\underline{y}) \phi_l({}^i\underline{y}) \tag{9}$$

and choosing the basis functions orthonormal according to this definition, we may diagonalize the linear equation system (8) and the coefficients a_l can be calculated independently by

$$a_l = \sum_{i=1}^{m} \left(1 - \frac{B({}^i\underline{y})}{p({}^i\underline{y})} \right) \frac{Z({}^i\underline{y})}{p({}^i\underline{y})} \phi_l({}^i\underline{y}), \tag{10}$$

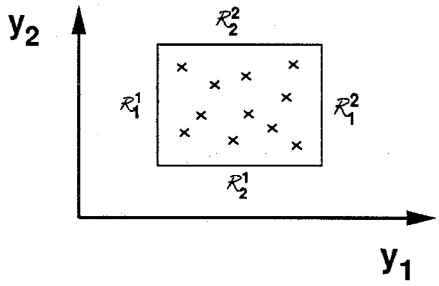

Figure 3. Cell with a set of reference points inside and boundary functions $b_i^j(\underline{y})$ on the boundaries $\mathcal{R}_i^j$.

until the accuracy is high enough.

The coefficients to build the basis functions $\phi_j(y)$ from the monomials $(1, y_1, y_2, \ldots, y_N, y_1^2, y_1y_2, y_2^2, \ldots, y_N^2, y_1^3, \ldots)$ are calculated in parallel to the expansion of the series $L(y)$ by the Gram–Schmidt-orthogonalization procedure [27]. The well-known instability of the Gram–Schmidt process is not crucial in this application, because instead of calculating high-order polynomials, we reduce the size of the coarse cells, which results in a smaller number of necessary basis functions that have to be orthogonalized. At this point it turns out to be numerically advantageous to choose the local coordinates in the range from -1 to 1 in each dimension.

Another advantage of this scheme is the large amount of freedom in choosing the reference points $p({}^i\underline{y})$ to adjust the approximating polynomial. In principle, no regular pattern is needed, as it is sketched in Figure 3. If there are numerical problems in calculating a reference point at some local coordinates ${}^i\underline{y}$ (*e.g.* a point may be outside of the range of existence of the manifold), this point $p({}^i\underline{y})$ can be rejected without causing any problems. But for a reliable outcome of the approximation, a homogeneous distribution of reference points should be achieved. In the current implementation, the sample points $p({}^i\underline{y})$ are calculated on regular meshes, which is demonstrated in Figure 4. The first point to be calculated is the one in the middle of the cell. By this, 2^N sub-cells are defined. The next points to be calculated are the mid-points of these sub-cells. This process of defining minor sub-cells and evaluation of mid-points can be continued, until there are sufficient reference points. The number of calculated reference points m is adjusted automatically to the number of used monomials k. In this way unphysical waves and oscillations in the approximating polynomial can be avoided. In the current implementation the grid is refined one level by calculation of additional points, when $m < 3k$. After calculating the coefficients of $B(\underline{y})$, $Z(\underline{y})$ and $L(\underline{y})$ we observe that they form one resulting polynomial $F(\underline{y})$. These coefficients are tabulated.

2.3.3. *Calculation of the boundary-element-functions*

Up to this point the calculation of the boundary-element-functions $b_i^j(\underline{y})$ has not been mentioned. They are calculated by the same algorithm according to *ansatz* (4) in one lower dimension. Here the same problem of the sub-element boundary functions arises. Each N-dimensional cell has σ_N^i i-dimensional boundaries S_j^i $(j = 1, 2, \ldots, \sigma_N^i)$, where

$$\sigma_N^i = \frac{N!}{i!(N-i)!}2^{N-i}. \tag{11}$$

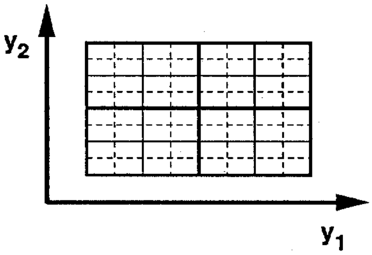

Figure 4. Grid of reference points with 3 levels of refinement.

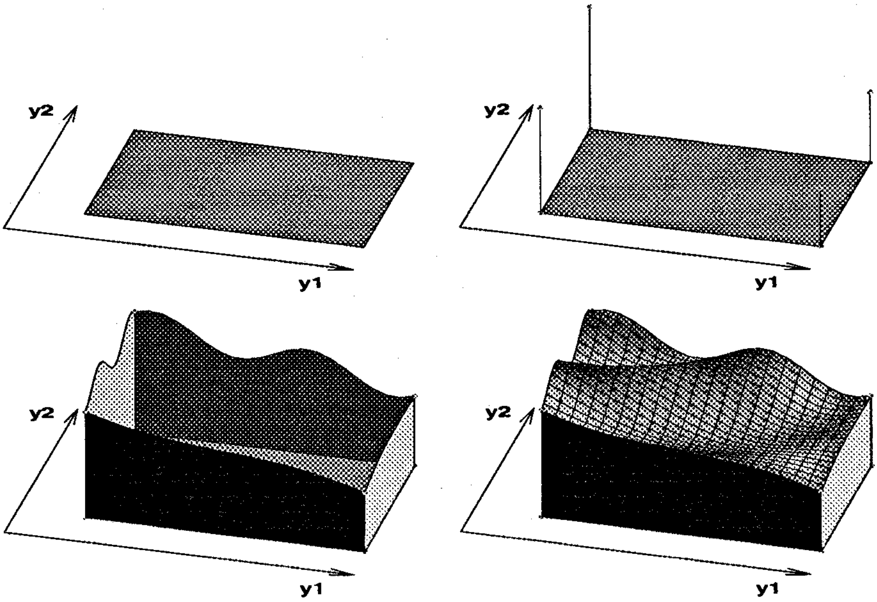

Figure 5. Idea of fitting algorithm in a two-dimensional example: (1) Setup of rectangular cell. (2) Evaluation of the values at the corners of the cell. (3) Fitting of the one-dimensional boundaries of the two-dimensional cell. (4) Fitting of the two-dimensional inner area of the cell.

Thus, a 2-dimensional cell has $\sigma_2^0 = 4$ corner points and $\sigma_2^1 = 4$ bounding edges, a 3-dimensional cell has $\sigma_3^0 = 8$ corner points, $\sigma_3^1 = 12$ bounding edges, and $\sigma_3^2 = 6$ bounding surfaces. For the set-up of the boundary functions we perform a sweep through the dimensions (see Figure 5)

(1) Start with the σ_N^0 corner points $\mathcal{S}_j^0$ of the cell, and use the values as boundary-element functions to calculate the approximating functions on the σ_N^1 bounding edges $\mathcal{S}_j^1$.

(2) Use the approximating functions on these bounding edges as boundary functions to calculate the approximating functions on the the σ_N^2 bounding surfaces $\mathcal{S}_j^2$.

(3) Continue this process until the approximating function in the cell (σ_N^N) has been calculated from the boundary functions defined by the approximating functions on the hyperplanes (σ_N^{N-1}).

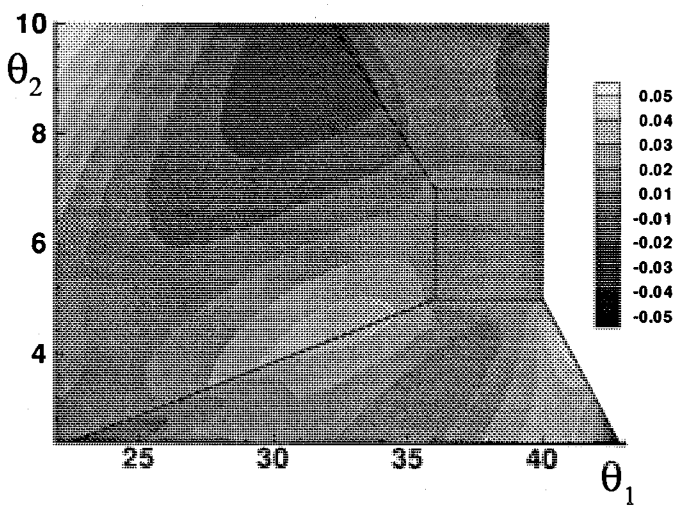

Figure 6. Relative approximation error for the mass fractions of OH radicals for the ILDM of a stoichiometric H_2-O_2-system.

3. Application to the ILDM of a stoichiometric H_2-O_2 system

We shall now demonstrate and verify the new tabulation method, using the ILDM of a stoichiometric hydrogen-oxygen system [17]. In this example 52 properties are tabulated in terms of two reaction-progress variables $(\theta_1 = w_{H_2O}/M_{H_2O}, \theta_2 = w_H/M_H)$. The set-up of the coarse grid has been done by hand. A small cell has been inserted near the equilibrium value to allow a high resolution of the reaction rates near equilibrium. (*cf.* Figure 1). The error tolerance (average relative error) for the fitting procedure was set to 0·05. Having in mind the usual uncertainty of kinetic data, we observe that this accuracy is high enough for practical calculations. But, of course, the accuracy can be increased if necessary. The grade of the approximating polynomial is adapting automatically to match the desired accuracy. For this application the resulting grade changes from constant monomials up to grade-5 polynomials. Most properties are fitted by grade-3 polynomials.

In Figure 6 the relative approximation errors for the mass fractions of OH-radicals are shown as contours. The small cell contains the domain around the chemical equilibrium where enhanced accuracy is needed. It can be seen that the equilibrium region is approximated with high accuracy. This is desirable for the application in CFD-codes, due to the high sensitivity of the CFD-results on the used chemistry near the equilibrium value. Furthermore it can be seen from Figure 6 that the relative error at the cell boundaries is continuous and vanishes at the cell corners. Thus, it is shown that the algorithm produces fitting polynomials with the desired continuity between the cells. In addition, Figure 6 shows the smooth and well-behaved property of the fitting. The highest relative errors are in the range of the pre-defined average error tolerance and no artificial oscillations (known from simple polynomial approximations) are produced. This is expected, because a least-squares approach, involving far more reference points than coefficients to be fitted, is used.

The computing time for the polynomial storage scheme is of the order of a few minutes. Compared to the time for the calculation of the manifold itself, this is negligible. On the other hand, the storage requirement for the ILDM is reduced dramatically if the polynomial

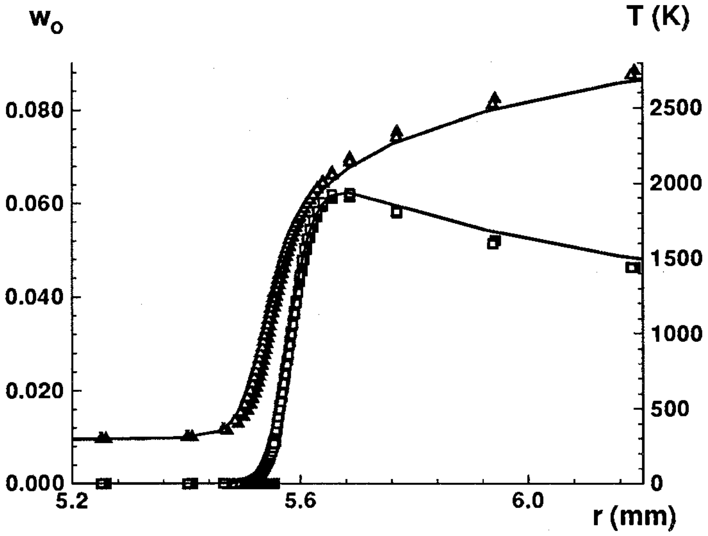

Figure 7. Profiles of temperature (Δ) and O-radicals (□) in a premixed laminar H_2-O_2 flame. The lines denote computation with detailed and the symbols with reduced chemistry. (Full symbols: standard look-up table, Empty symbols: new polynomial table).

approximation is used. The table with the old storage scheme needs about 15 Mbytes of storage, whereas the new table does only occupy about 80 Kbytes.

The results presented above show the improvement of the new scheme compared with our previously used storage scheme [16]. In order to verify the approach and its implementation in CFD-codes further, we performed laminar flat-flame calculations for a stoichiometric hydrogen-oxygen system (*cf.* [17]). In the flat-flame code the table look-up procedure has been replaced by a subroutine that evaluates the polynomial approximations. We performed calculations of flame profiles for detailed chemistry, as well as for ILDM-reduced chemistry using both storage schemes. The computation time is reduced drastically by the use of ILDM-reduced chemistry for both storage schemes. In comparison with the old tabulation, the new polynomial tabulation scheme does not affect the computation time significantly. Figures 7–9 show temperature and various species profiles in the flame. Temperature, major species H_2 and H_2O, and minor species like O, OH and H are reproduced very well by the reduced schemes. There is no significant difference between the two storage schemes, which is very promising, because, on the other hand, the storage requirement is reduced by a factor of 200 when the new polynomial approximation is used.

4. Conclusions

In most practical reacting-flow calculations the direct use of detailed chemistry is computationally prohibitive. Thus, reduced chemical-kinetics schemes are devised, which allow to describe the chemical system in terms of a small number of reaction-progress variables, and very often the information on the chemical kinetics (*e.g.*, reaction rates) is calculated

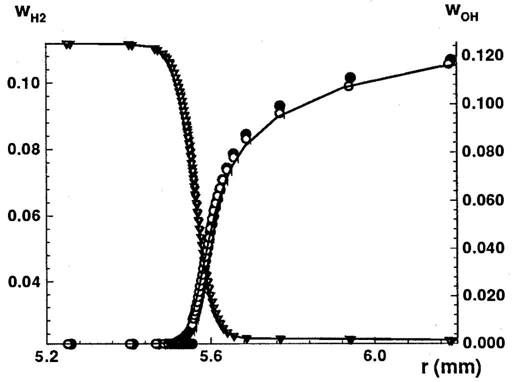

Figure 8. Profiles of H_2 (∇) and OH-radicals ($\circ$) in a premixed laminar H_2O_2 flame. The lines denote computation with detailed and the symbols with reduced chemistry. (Full symbols: standard look-up table, Empty symbols: new polynomial table).

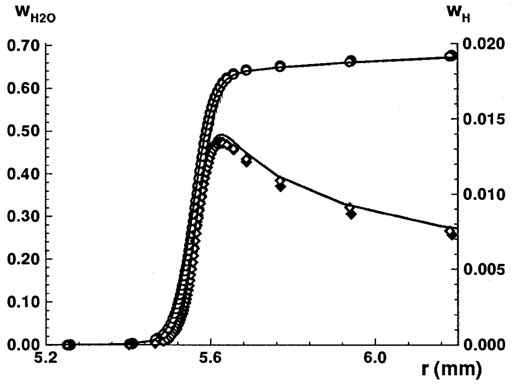

Figure 9. Profiles of H_2O ($\circ$) and H-radicals ($\diamond$) in a premixed laminar H_2-O_2 flame. The lines denote computation with detailed and the symbols with reduced chemistry. (Full symbols: standard look-up table, Empty symbols: new polynomial table).

beforehand and stored for the CFD-calculation. We have developed a storage scheme based on orthogonal polynomials. Instead of using a locally refined tabulation grid, together with multi-linear interpolation within the grid cells [16], we divide the domain into a small number of coarse cells and use polynomial approximations within these cells. Special methods assure that the polynomial approximations are not only continuous within the coarse cells, but all over the domain. The storage requirement is reduced considerably. In order to verify the approach, we performed calculations of laminar premixed flat-flame calculations for a stoichiometric hydrogen-oxygen system, using both detailed and ILDM-reduced chemistry. In this specific example the storage requirement is reduced by a factor of 200. However, the storage procedure is not restricted to this use in combination with ILDM-reduced chemistry. Other applications of storage schemes are, *e.g.*, the storage of pre-integrated reaction rates for turbulent flame calculations [28] or the storage of laminar flamelet libraries [29]. For such applications the polynomial storage scheme might also be used.

Acknowledgments

The authors would like to thank T. Turanyi for bringing the advantages of storage schemes based on orthogonal polynomials to their attention. Financial support by the CEC (in the frame of the BRITE/EURAM-Project) and the *BMFT* (in the frame of the TECFLAM-Project) is gratefully acknowledged.

References

1. J. Warnatz, Resolution of gas phase and surface chemistry into elementary reactions. 24th Symposium (International) on Combustion. Pittsburgh: The Combustion Institute (1992) pp. 553–579.
2. U. Maas and J. Warnatz, Simulation of chemically reacting flows in two-dimensional geometries. *IMPACT Comp. Sci. Eng.* 1 (1989) 394–420.
3. J. Warnatz, U. Maas and R.W. Dibble, *Combustion*. Berlin-Heidelberg-New York: Springer-Verlag (1996) 265 pp.
4. S.B. Pope, Computations of turbulent combustion: Progress and challenges. 23rd Symposium (International) on Combustion. Pittsburg: The Combustion Institute (1990) pp. 591–612.
5. N. Peters, Laminar flamelet concepts in turbulent combustion. 21st Symposium (International) on Combustion. Pittsburg: The Combustion Institute (1986) pp. 1231–1250.

6. P.A. Libby and F.A. Williams (eds.), *Turbulent Reactive Flows*. New York: Springer (1980) 243 pp.
7. C. Chevalier, *Entwicklung eines detaillierten Reaktionsmechanismus zur Modellierung der Verbrennungsprozesse von Kohlenwasserstoffen bei Hoch- und Niedertemperaturbedingungen*. PhD thesis, Institut für Technische Verbrennung, Universität Stuttgart (1993) 218 pp.
8. M. Bodenstein, Geschwindigkeit der Bildung des Bromwasserstoffs aus seinen Elementen. *Z. Phys. Chem.*, 57 (1906) 168–175.
9. N. Peters and B. Rogg, *Reduced Kinetic Mechanisms for Applications in Combustion Systems*. Berlin: Springer (1993) 360 pp.
10. J.C. Keck, Rate-controlled constrained equilibrium calculations of ignition delay times in hydrogen–oxygen mixtures. 22nd Symposium (International) on Combustion. Pittsburg: The Combustion Institute (1988) pp. 1705–1713.
11. S.H. Lam and D.A. Goussis, Understanding complex chemical kinetics with computational singular perturbation. 22nd Symposium (International) on Combustion. Pittsburg: The Combustion Institute (1988) pp. 931–941.
12. S.H. Lam and D.A. Goussis, *Conventional Assymptotics and Computational Singular Perturbation for Simplified Kinetics Modelling*. Technical report, Princeton University, USA. Technical Report 1864(a)-MAE (1990) 94 pp.
13. F.C. Christo, A.R. Masri, E.M. Nebot and T. Turanyi, Utilising artificial neural network and repro-modelling in turbulent combustion. Proc. of the IEEE Symposium on Artificial Neural Networks, Perth (1995) pp. 911–916.
14. P. Deuflhard and J. Heroth, Dynamic dimension reduction in ODE models. Technical report, Konrad–Zuse–Zentrum für Informationstechnik Berlin, Preprint SC95-29 (1995) 16 pp.
15. U. Maas and S.B. Pope, Simplifying chemical kinetics: Intrinsic low-dimensional manifolds in composition space. *Combustion and Flame* 88 (1992) 239–264.
16. U. Maas and S.B. Pope, Implementation of simplified chemical kinetics based on intrinsic low-dimensional manifolds. 24th Symposium (International) on Combustion. Pittsburg: The Combustion Institute (1992) 103–112.
17. U. Maas and S.B. Pope, Laminar flame calculations using simplified chemical kinetics based on intrinsic low-dimensional manifolds. 25th Symposium (International) on Combustion. The Combustion Institute, Pittsburg, 1994.
18. M.D. Smooke (ed.), Reduced kinetic mechanisms and asymptotic approximations for methane-air flames. *Lecture Notes in Physics* 384. Berlin-Heidelberg-New York: Springer (1991) 245 pp.
19. A.S. Tomlin, T. Turanyi and M.J. Pilling, *Oxidation Kinetics and Autoignition of Hydrocarbons*. Elsevier, in press.
20. U. Maas, Coupling of chemical reaction with flow and molecular transport. *Applications of Mathematics* 3 (1995) 249–266.
21. U. Maas, *Automatische Reduktion von Reaktionsmechanismen zur Simulation reaktiver Strömungen*. Habilitation Thesis, Institut für Technische Verbrennung, Universität Stuttgart (1993) 155 pp.
22. D. Schmidt, U. Maas and J. Warnatz, Simplifying chemical kinetics for the simulation of hypersonic flows using intrinsic low-dimensional manifolds. Proc. of the 5th International Symposium on Computational Fluid Dynamics, Sendai, Japan (1993) pp. 81–86.
23. D. Schmidt, U. Maas, J. Segatz, U. Riedel and J. Warnatz, Simulation of laminar methane-air flames using automatically simplified chemical kinetics. *Comb. Sci. Tech.* 113-114 (1996) 3–16.
24. U. Riedel, D. Schmidt, U. Maas and J. Warnatz, Laminar flame calculations based on automatically simplified chemical kinetics. Proc. of the 35th Eurotherm Seminar, Compact Fired Heating Systems, Leuven, Belgium (1994) pp. 1–14.
25. T. Turanyi, Parameterization of reaction mechanisms using orthonormal polynomials. *Computers Chem.* 18 (1994) pp. 45–54.
26. B. Yang and S.B. Pope, A tree method for treating chemical reactions in PDF calculations of turbulent combustion. Proc. 6th International Conference on Numerical Combustion, New Orleans (1996) pp. 215–216.
27. I.N. Bronstein und K.A. Semendjajew, *Taschenbuch der Mathematik*. Leipzig: BSB B.G. Teubner Verlagsgesellschaft (1979) 860 pp.
28. A.T. Norris and S.B. Pope, Modeling of extinction in turbulent diffusion flames by the velocity-dissipation-composition pdf method. *Combustion and Flame* 100 (1995) 211–220.
29. J. Göttgens, F. Mauss and N. Peters, Analytic approximations of burning velocities and flame thickness of lean hydrogen, methane, ethylene, ethane, acetylen, and propane flames. 24th Symposium (International) on Combustion. Pittsburg: The Combustion Institute (1992) pp. 129–135.